Journal of Energy Chemistry 36 (2019) 1–6

Contents lists available at ScienceDirect

Journal of Energy Chemistry

journal homepage: www.elsevier.com/locate/jechem

http://www.journals.elsevier.com/journal-of-energy-chemistry/

Bismuth doped lead-free two-dimensional tin based halide perovskite single crystals

Ruiling Zhang[a,b,1], Xin Mao[a,b,1], Pengfei Cheng[a,b], Yang Yang[a], Songqiu Yang[a], Tuerdi Wumaier[c], Weiqiao Deng[a], Keli Han[a,*]

[a] State Key Laboratory of Molecular Reaction Dynamics, Dalian Institute of Chemical Physics, Chinese Academy of Sciences, Dalian 116023, Liaoning, China
[b] University of the Chinese Academy of Sciences, Beijing 100049, China
[c] Department of Physics, Xinjiang Institute of Engineering, Urumqi 830091, Xinjiang, China

Dedicated to the 70th anniversary of Dalian Institute of Chemical Physics, CAS, China.

ARTICLE INFO

Article history:
Received 22 October 2018
Revised 21 November 2018
Accepted 6 December 2018
Available online 10 December 2018

Keywords:
Heterovalent-metal doping
Photoluminescence
Self-trapped excitons
Femtosecond transient absorption spectra
Global analysis fit

ABSTRACT

Heterovalent-metal doping is an efficient tool to tune the optoelectronic properties of the famous halide perovskites. Previous studies have focused on the heterovalent-doping in three-dimensional (3D) halide perovskites. However, there is a lack of such doping in two-dimensional perovskites which possess unique optoelectronic properties and improved chemical stability as compared to 3D analogues. Here, we present successful doping of Bismuth into the lattice of lead-free, two-dimensional perovskite PEA_2SnBr_4 single crystals. Structural characterizations demonstrate that the doped crystals possess identical crystal structure and layered morphology with the pristine one. Intriguingly, we find the PL peak and spectral shape can be tailored by tuning the concentration of Bi dopants. Femtosecond transient absorption spectroscopy is performed to understand the underlying mechanism related to tunable PL behaviors, and a clear picture of the Bismuth-doping impact is provided.

Ke-Li Han's Group for Complex Molecular Systems Reaction Dynamics. Our research interests involve chemistry, physics, biology, and material sciences investigated by both theoretical and experimental methods applied in molecular reaction dynamics fields. Recently, we focus our studies on several important research areas such as: Excited-state dynamics of perovskites; Hydrogen Bonding Effects on the Photochemistry and Photobiology; Excited-State Structures and Dynamics of Complex Molecular Systems; Nonadiabatic Effects in Chemical Reaction; Chemical Reactions Catalyzed by Enzyme; Dynamical Mechanisms in Hydrogen Production by Photocatalytic Water Splitting and Solar Cells.

1. Introduction

Recently, heterovalent-metal doping, which is widely used in semiconductors for bandgap and conduction type engineering, has received intensive attention as an efficient method to tailor the optoelectronic properties of the famous organic-inorganic hybrid halide perovskites [1–11]. For instance, trivalent element Bi^{3+} doping into the lattice of $APbX_3$ ($A = CH_3NH_3$, Cs; X = I, Br, Cl) perovskites can enhance the light absorption at long-wavelength region [6,8,10,11]. It is noteworthy that most researchers have concentrated on the heterovalent doping in 3D lead halide perovskites. However, to the best of our knowledge, there is a lack of such investigations on two-dimensional (2D) perovskites. In fact, due to the inherent quantum confinement and low dielectric constant effect [12], 2D perovskites with improved moisture stability compared to 3D analogues, possess some unique properties [13–18], e.g. direct bandgap type and large exciton binding energy. Heterovalent doping can offer a route to tailor these special properties, and endow 2D perovskites with more potential applications in optoelectronic field. In addition, despite the superior properties of lead halide perovskites, the toxicity of Pb hinders their commercial potential. Thus, increasing attention has been focused on environmentally-friendly lead-free alternatives, in particular for Sn which comes from the same Group of periodic table with Pb [9,19–27].

In this regard, we focused on the effect of heterovalent-metal doping in two-dimensional Sn-based perovskites. Considering the unique role of Bi-doping in lead perovskites and the similar ionic radius of Bi^{3+} and Sn^{2+}, we synthesized a suite of Bi^{3+}-doped lead-free, two-dimensional perovskite $PEA_2Sn_{1-x}Bi_xBr_{4+x}$ ($x << 1$)

* Corresponding author.
E-mail address: klhan@dicp.ac.cn (K. Han).
[1] Both the authors contributed equally to this paper.

https://doi.org/10.1016/j.jechem.2018.12.003

single crystals. The characterization techniques including powder X-ray, scanning electron microscope (SEM), steady-state diffuse reflection and photoluminescence (PL) spectroscopies were used to determine the crystal structure and optical properties. Interestingly, we find that the photoluminescence spectra can be tailored by tuning the concentration of Bi^{3+}. To elucidate the underlying mechanism, femtosecond transient absorption (fsTA) spectroscopy was performed. We propose that both of free excitons (FEs) and intrinsic self-trapped excitons (STEs) contribute to the PL of pristine crystals, and incorporation of Bi^{3+} can prompt the formation of extrinsic self-trapped excitons, which play a significant role in tailoring PL behaviors.

2. Experimental

2.1. Preparation of $PEA_2Sn_{1-x}Bi_xBr_{4+x}$ single crystals

Single crystals were fabricated by cooling-induced crystallization method. PEA_2SnBr_4 was prepared by mixing 1 mmol $C_6H_5CH_2CH_2NH_3Br$ (PEABr) and 0.5 mmol $SnBr_2$ in 3 mL of HBr (48% w/w aq. soln.) and 3 mL of H_3PO_2 (50% w/w aq. soln.). For $PEA_2Sn_{1-x}Bi_xBr_4$, the required amount x of $BiBr_3$ was added to the solution. The solution was stirred at 120 °C for 1 h, turning to a clear solution. Then the stirring was stopped, and the solution was cooled to room temperature to afford yellow flake-like crystals for PEA_2SnBr_4 and black flake-like crystals for Bi-doped PEA_2SnBr_4. The general procedures mentioned above were done in a N_2 atmosphere. Finally the crystals were washed with a minimum quantity of dried ethanol and dried in vacuum at 60 °C for 12 h.

2.2. Characterization

PANalytical Empyrean using Cu $K\alpha$ radiation ($\lambda = 1.54056$ Å) was conducted with every 0.04° increment over the Bragg angle range of 5°–70° for X-ray analysis at room temperature. The molar ratio of Bi in crystals was determined by Perkin Elmer 7300 DV inductively coupled plasma-optical emission spectroscopy (ICP-OES). The optical diffuse reflectance spectra of samples were measured by a Shimadzu Uv 2550 spectrometer equipped with an integrating sphere over the spectral range 200–900 nm at room temperature. $BaSO_4$ was used as blank reference. PL spectra were recorded on the Horiba PTI QuantaMaster 400. A field emission scanning electron microscope (FESEM, JEOL, JSM-7800F, 1 kV) equipped with an Oxford X-Max silicon drift detector was used to record the surface morphology analysis and perform chemical analysis. The PLQE measurement was performed using an absolute PL quantum yield spectrometer (Hamamatsu C11347).

2.3. Femtosecond transient absorption (FsTA) measurement

Femtosecond transient absorption measurements were performed by a pump-probe laser system (800 nm, 50 fs, and 1 kHz repetition rate) based on a regenerative amplified Ti: sapphire laser source (Spectra Physics). The sample was excited by 350 nm laser pulses generated by a TOPAS Optical Parametric Amplifier (OPA) which was pumped by the 800 nm pulse. A white light continuum (WLC) generated by a 2 mm thick CaF_2 with window from 350 to 800 nm was used as the probe beam. The delay between the pump and probe pulse was controlled by a motorized delay stage. The resulting data were analyzed by global analysis with the graphical interface program Glotaran [28]. Global analysis with a parallel model was performed to yield decay-associated difference spectra (DADS) [29]. The sample was prepared by mechanically grinding single crystals using two quartz plates.

3. Results and discussion

3.1. Morphology of $PEA_2Sn_{1-x}Bi_xBr_{4+x}$ single crystals

Firstly, we analyze the macroscopic morphology of crystals by combination of SEM and energy dispersive X-ray spectroscopy (EDS) experiments. As shown in Fig. 1(a) and (b), for pristine PEA_2SnBr_4 [30], the inorganic $[SnBr_6]^{4-}$ octahedron sheets are sandwiched by large organic cations PEA^+, leading to a characteristic layered morphology of two-dimensional perovskites (Fig. 1(c)). Bi^{3+} doping retains the layered feature of PEA_2SnBr_4, but changes the crystal color from yellow to black (Fig. 1(d)). The corresponding EDS spectra are provided in Figs. S1 and S2, and confirm the presence of Bismuth in the doped PEA_2SnBr_4. To get the accurate doping ratio in crystals, ICP-OES measurements were conducted, and a linear relationship of the dopant concentration in feed solution and single crystals was obtained (Fig. S3). The accurate Bi molar ratio for 10% Bi-doped PEA_2SnBr_4 is 0.7%. In the following, the samples are denoted by the Bi molar concentration in feed solution for clarity. With increasing the Bi concentration from 1% to 20% in feed solution, the diffraction peaks of XRD show no obvious shift, which may result from the similar ionic radiuses of Sn^{2+} and Bi^{3+} cations (Fig. S4a). But Bi-doping influences the relative intensity of the diffraction peaks of XRD (Fig. S4b).

3.2. Steady-state diffuse reflection and photoluminescence spectra

Subsequently, UV–vis diffuse reflectance and PL spectroscopies were performed to investigate the optical properties of Bi-doped crystals. As shown in Fig. 2(a), the bandgap of pristine PEA_2SnBr_4 is estimated to be 2.60 eV, which is consistent with the previous report [30]. With increasing dopant concentration from 0% to 20%, no obvious change of bandgap is observed, but the absorption band tail becomes gradually increased. Such result has been reported in Bi-doped $MAPbBr_3$ [31]. The incremental absorption band tail is considered to be the Urbach tail, which can be induced by lattice distortion and self-trapped exciton absorption [32–34]. Due to the quantum confinement and low dielectric effect, 2D perovskites possess high exciton binding energy typically above 300 meV [12–15,35]. An excitonic absorption peak at around 440 nm was observed for both of undoped and doped PEA_2SnBr_4.

Interesting phenomenon was observed in PL spectra of a suite of Bi-doped crystals. As shown in Fig. 2(b), all the PL spectra can be well fitted by one and two Lorentz distributions, respectively. The PL spectrum of undoped PEA_2SnBr_4 is characterized by an asymmetric line-shape, tailing to longer wavelength and can be well fitted by two peaks. Furthermore, a narrower PL spectrum was observed at 77 K (Fig. S5b). According to the previous reports [14,36–39], the higher energy emission is ascribed to free excitons transition and the lower energy tail is tentatively assigned to radiative recombination of self-trapped excitons. Additional powerful evidence comes from the fsTA spectra as discussed below. With increasing the Bi concentration from 0% to 20%, the change of spectra shows two obvious features: (1) the PL peaks are blue-shifted from 495 to 472 nm; (2) the lower energy emission tail gradually attenuates and is disappeared in 10% and 20% Bi-doped crystals. In addition, Bi doping weakens the emission intensity of the pristine crystal. The PL quantum yield of 10% Bi-doped crystal is shortened from 0.5% to 0.3% as compared to the undoped one. The blue shift of PL spectra in doped perovskite crystals has also been observed in Bi-doped $MAPbBr_3$ perovskite and ascribed to photon recycling [31,40,41]. Considering that the observed PL spectra are the combination of FEs and STEs transitions, and the blue shift of PL spectra is derived from not only the photon recycling effect, but also the quenching of radiative self-trapped states induced by incorporation

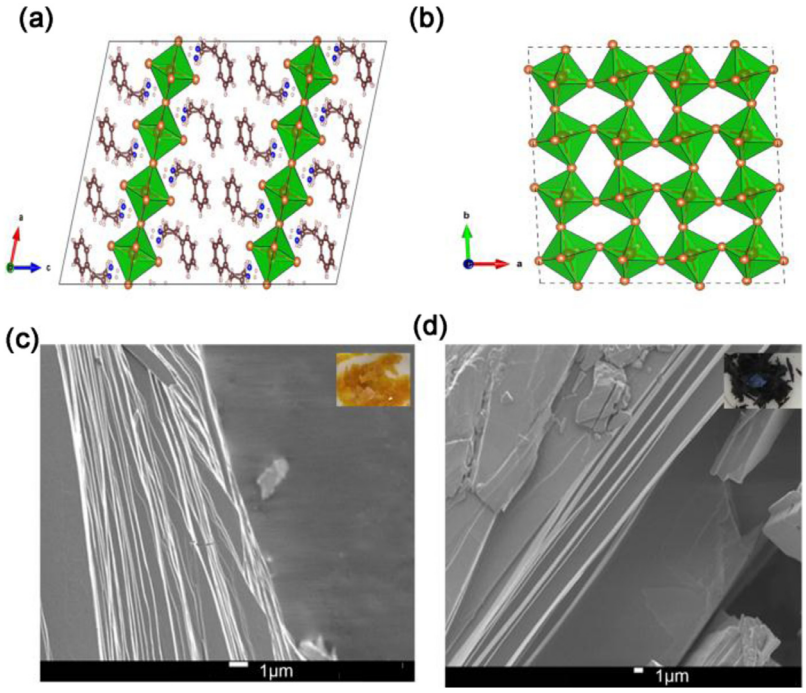

Fig. 1. (a) Crystal structural illustration of PEA_2SnBr_4 viewed along the b axis. Brown, white, blue, red, orange spheres represent C, H, N, Sn, Br atoms, respectively. (b) Distorted $[SnBr_6]^{4-}$ octahedron viewed along c axis. SEM images of PEA_2SnBr_4 single crystals (c) and 10% Bi-doped PEA_2SnBr_4 single crystals (d). Insets are the corresponding single crystal photos.

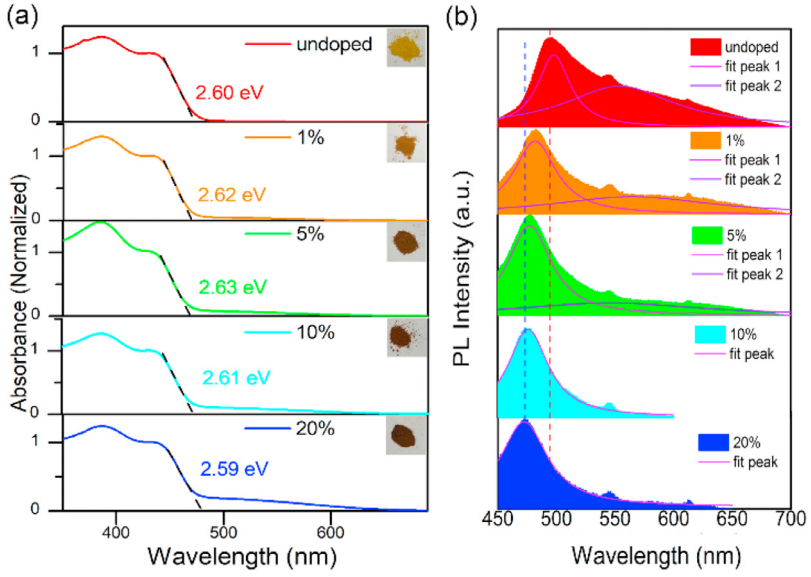

Fig. 2. Optical diffuse reflectance spectra (a), and room temperature PL spectra (b) of Bi-doped PEA_2SnBr_4 with different Bi concentrations ranging from 0% to 20% in the feed solution. Insets are the corresponding powder photos.

of Bi^{3+}. To further prove this inference, femtosecond transient absorption spectroscopy was carried out.

3.3. Femtosecond transient absorption spectra

The fsTA spectra of undoped and 10% Bi-doped PEA_2SnBr_4 crystals were measured upon above-excitonic-peak excitation at 350 nm. Transient absorption spectroscopy is an efficient tool to give the most direct evidence for self-trapped excitons, and a pump-induced absorption at energies below that of excitons is characteristic of STEs [42,43]. As shown in Fig. 3(a), following photoexcitation, the TA spectra of PEA_2SnBr_4 are dominated by a negative signal corresponding to the ground-state bleaching at the optical gap around 440 nm, and a positive absorption at energies below that of excitons, which is characteristic of STEs [42–44]. The TA spectra confirm the presence of STEs and are consistent with the above PL results. Notably, the STE characteristic absorption is not only observed in the fsTA spectra of doped crystals (Fig. 3(d)) but also stronger than that of undoped crystals (Fig. 3(c)). This suggests that more STEs are generated in Bi-doped PEA_2SnBr_4. It is known that there are two types of STEs: intrinsic one which results from transient lattice distortions and doesn't require permanent material defects, and extrinsic one which is attributed to the local heterogeneity of the lattice (impurity) [43,45,46].

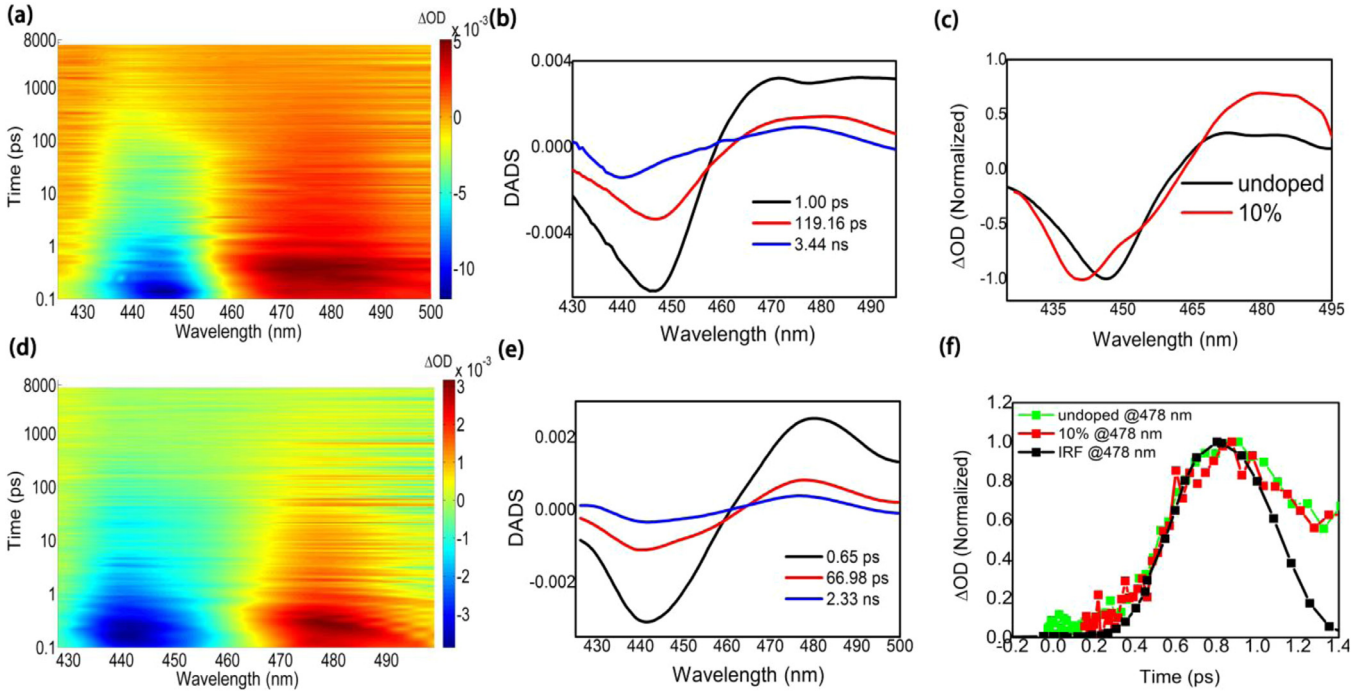

Fig. 3. Contour plot of the fsTA spectra upon photoexcitation at 350 nm with time window from 0 to 7800 ps (a), and DADS spectra derived from global analysis (b) of PEA_2SnBr_4. (c) Normalized fsTA spectra at decay time of 170 fs for undoped and 10% Bi-doped PEA_2SnBr_4. The contour plot of the fsTA spectra upon photoexcitation at 350 nm with time window from 0 to 7800 ps (d), and DADS spectra derived from global analysis (e) of 10% Bi-doped PEA_2SnBr_4. (f) Normalized kinetic profiles of undoped and 10% Bi-doped PEA_2SnBr_4 and instrumental response function (IRF) at 478 nm. The excitation energy is 4 μJ/cm^2/pulse.

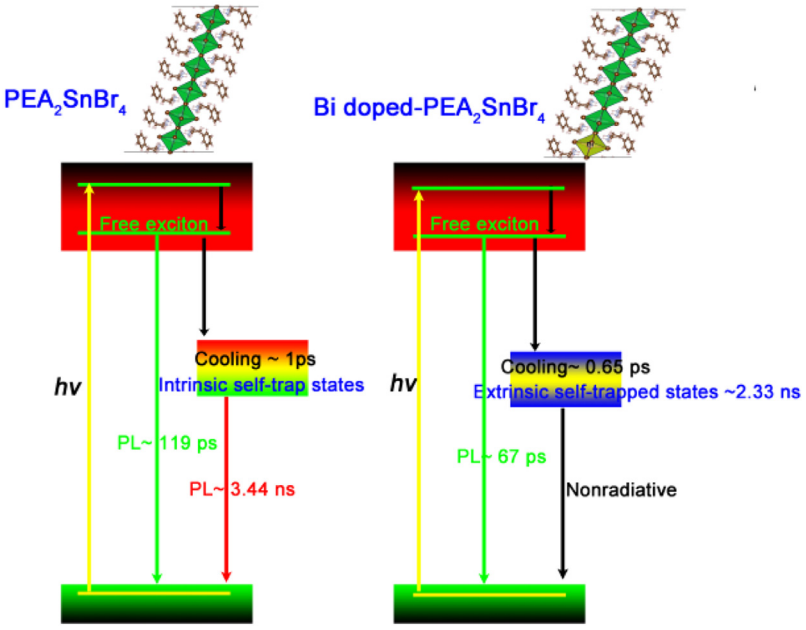

Fig. 4. Excited-state dynamics model of undoped and 10% Bi-doped PEA_2SnBr_4.

Therefore, we assign the STEs in pristine PEA_2SnBr_4 crystal to intrinsic self-trapped excitons, and ascribe the pump-induced absorption of 10% Bi-doped PEA_2SnBr_4 to the formation of extrinsic self-trapped excitons. Both of the formation time of the two STEs determined from the rise time of the pump-induced absorption, are within the instrumental response resolution (~100 fs) (Fig. 3(f)). In consideration of the absence of lower energy emission in Bi-doped PEA_2SnBr_4 as discussed above, we propose that extrinsic STEs in doped crystals relax in a nonradiative way.

Global analysis with a parallel kinetic model was performed on the fsTA spectra to yield decay associated difference spectra (DADS) (Fig. 3(b) and (e)). For undoped and 10% Bi-doped PEA_2SnBr_4 crystals, both of ground-state bleaching and excited-state absorption signals decay to zero in the time window of 7.8 ns in this experiment (Fig. S7). Both of their spectra can be well global fitted by three components (Fig. 3(b) and (e)) and the corresponding time constants are summarized in Table S1. An ultrafast component of 1 ps for PEA_2SnBr_4 and 0.65 ps for 10% Bi-doped

PEA_2SnBr_4 is observed. To rule out the possibility of Auger combination which is an ultrafast process in high carrier density, we use low excitation energy of 4 μJ/cm^2/pulse. We also compare the kinetic profiles at 478 nm of 10% Bi-doped PEA_2SnBr_4 with different excitation energies (Fig. S6). The same decay behaviors also confirm the absence of Auger combination process at the present experiment condition [47]. We tentatively ascribe the ultrafast process to the cooling of relaxed self-trapped states [46,48,49]. It is shown that the relaxation of the hot trap states ($\tau_2 = 0.65$ ps) is faster in Bi-doped PEA_2SnBr_4 compared to that ($\tau_2 = 1$ ps) in pristine crystals. Considering that the PL of PEA_2SnBr_4 comes from the radiative combination of free excitons and intrinsic self-trapped excitons as discussed above, the short-lived component with lifetime of 119 ps is ascribed to the radiative decay of free excitons, and the long-lived component with lifetime of 3.44 ns is associated with the decay of the intrinsic self-trapped excitons. The two lifetimes obtained by fsTA spectra are consistent with that measured by time-resolved photoluminescence spectroscopy in the previous report [50]. Different from the long lifetime of spin-triplet STEs in the previous report [24], the short lifetime in nanoseconds indicates the spin-singlet character. Similarity, for 10% Bi-doped PEA_2SnBr_4, the lifetimes of free excitons and extrinsic self-trapped excitons are 66.92 ps and 2.33 ns, respectively. The quenching ratio of free excitons by incorporation of Bi is estimated to be 44% (see details in supporting information), which accounts for the weaker PL intensity of 10%Bi-doped in PEA_2SnBr_4.

Hence, by using femtosecond transient absorption spectroscopy, we confirm the inference about PL spectra as discussed above. As shown in Fig. 4, for pristine PEA_2SnBr_4, upon photoexcitation, free excitons emerge due to the high exciton binding energy of two-dimensional perovskites. Some free excitons combine radiatively and some are trapped by deformable lattice, forming radiative intrinsic self-trapped excitons. Both of them lead to an asymmetric line-shape of PL spectra. For 10% Bi-doped PEA_2SnBr_4, the extrinsic self-trapped excitons are generated due to the local heterogeneity of the lattice induced by incorporation of Bi. These extrinsic self-trapped states are nonradiative and contribute to the enhanced absorption tail. Both of photon recycling and nonradiative extrinsic self-trapped states lead to tunable PL spectra of Bi-doped PEA_2SnBr_4 crystals.

4. Conclusions

We synthesized a suite of Bi-doped lead-free two-dimensional perovskites $PEA_2Sn_{1-x}Bi_xBr_{4+x}$ ($x << 1$) single crystals, and observed tunable PL behaviors by tuning the dopant concentration. By using femtosecond transient absorption spectroscopy, we propose that the incorporation of Bi can promote the formation of nonradiative extrinsic self-trapped excitons, which play a significant role in PL tailoring. Our work not only fills the missing links of the present status of our knowledge about the heterovalent doping in two-dimensional lead-free halide perovskites, but also provides unique perspective on the role of Bi as a dopant.

Associated content

Supporting information. Experimental details; EDS of undoped and doped PEA_2SnBr_4; Bi molar concentration determined by ICP-OES and powder XRD of a suite of Bi-doped PEA_2SnBr_4; Comparison of stimulated and experimental powder XRD for PEA_2SnBr_4; TGA data of undoped and 10% Bi-doped PEA_2SnBr_4; XRD data of undoped and 10% Bi-doped PEA_2SnBr_4 for stability test; PL spectra of PEA_2SnBr_4 at 77 K; fsTA spectra of undoped and doped 10% Bi-doped PEA_2SnBr_4; Summary of time constants of fsTA spectra derived from global fits.

Notes

The authors declare no competing financial interests.

Acknowledgments

The work is supported by the National Key Research and Development Program of China (Grant No: 2016YFE0120900 and 2017YFA0204800), the National Natural Science Foundation of China (No. 21,703,244, 21,403,226, and 21,533,010), DICP DMTO201601, DICP ZZBS201703, the Science Challenging Program (JCKY2016212A501). DICP Outstanding Postdoctoral Foundation (2016YB09) and the China Postdoctoral Science Foundation (2017M611276).

Supplementary materials

Supplementary material associated with this article can be found, in the online version, at doi:10.1016/j.jechem.2018.12.003.

References

[1] H. Shao, X. Bai, H.N. Cui, G.C. Pan, P.T. Jing, S.N. Qu, J.Y. Zhu, Y. Zhai, B. Dong, H.W. Song, Nanoscale 10 (2018) 1023–1029.
[2] G.C. Pan, X. Bai, D.W. Yang, X. Chen, P.T. Jing, S.N. Qu, L.J Zhang, D.L. Zhou, J.Y. Zhu, W. Xu, B. Dong, H.W. Song, et al., Nano Lett 17 (12) (2017) 8005–8011.
[3] M. Liu, G.H. Zhong, Y.M. Yin, J.S. Miao, K. Li, C.Q. Wang, X.R. Xu, C. Shen, H. Meng, Adv. Sci. 4 (2017) 1700335.
[4] J.T. Wang, Z.P. Wang, S. Pathak, W. Zhang, D.W. deQuilettes, F. Wisnivesky-Rocca-Rivarola, J. Huang, P.K. Nayak, J.B. Patel, H.A.M. Yusof, et al., Energy Environ. Sci. 9 (2016) 2892–2901.
[5] Y.Q. Hu, T. Qiu, F. Bai, X.L. Miao, S.F. Zhang, J. Mater. Chem. A 5 (2017) 25258–25265.
[6] R.Q. Wang, X. Zhang, J.Q. He, C. Ma, L. Xu, P. Sheng, F.Q. Huang, J. Alloy. Compd. 695 (2017) 555–560.
[7] J. Zhang, M.H. Shang, P. Wang, X.K. Huang, J. Xu, Z.Y. Hu, Y.J. Zhu, L.Y. Han, ACS Energy Lett. 1 (2016) 535–541.
[8] R. Begum, M.R. Parida, A.L. Abdelhady, B. Murali, N.M. Alyami, G.H. Ahmed, M.N. Hedhili, O.M. Bakr, O.F. Mohammed, J. Am. Chem. Soc. 139 (2) (2017) 731–737.
[9] H. Hasegawa, K. Kobayashi, Y. Takahashi, J. Harada, T. Inabe, J. Mater. Chem. C 5 (2017) 4048–4052.
[10] Z. Zhang, L.X. Ren, H. Yan, S.J. Guo, S.H. Wang, M. Wang, K.X. Jin, J. Phys. Chem. C 121 (32) (2017) 17436–17441.
[11] A.L. Abdelhady, M.I. Saidaminov, B. Murali, V. Adinolfi, O. Voznyy, K. Katsiev, E. Alarousu, R. Comin, I. Dursun, L. Sinatra, et al., J. Phys. Chem. Lett. 7 (2) (2016) 295–301.
[12] X. Hong, T. Ishihara, A.V. Nurmikko, Phys. Rev. B 45 (12) (1992) 6961.
[13] L. Yuan, T. Wang, T. Zhu, M.W. Zhou, L.B. Huang, J. Phys. Chem. Lett. 8 (14) (2017) 3371–3379.
[14] M.D. Smith, A. Jaffe, E.R. Dohner, A.M. Lindenberg, H.I. Karunadasa, Chem. Sci. 8 (2017) 4497–4504.
[15] L. Pedesseau, D. Sapori, B. Traore, R. Robles, H.H. Fang, M.A. Loi, H.H. Tsai, W.Y. Nie, J.C. Blancon, A. Neukirch, et al., ACS Nano 10 (11) (2016) 9776–9786.
[16] Y.N. Chen, Y. Sun, J.J. Peng, J.H. Tang, K.B. Zheng, Z.Q. Liang, Adv. Mater. 30 (2018) 1703487.
[17] A. Raja, A. Chaves, J. Yu, G. Arefe, H.M. Hill, A.F. Rigosi, T.C. Berkelbach, P. Nagler, C. Schuller, T. Korn, et al., Nat. Commun. 8 (2017) 15251.
[18] J.X. Liu, J. Leng, K.F. Wu, J. Zhang, S.Y. Jin, J. Am. Chem. Soc. 139 (4) (2017) 1432–1435.
[19] S.Y. Shao, J. Liu, G. Portale, H.H. Fang, G.R. Blake, G.H. ten Brink, L.J.A. Koster, M.A. Loi, Adv. Energy Mater. 8 (2018) 1702019.
[20] C. Zhang, L.G. Gao, S.Z. Hayase, T.L. Ma, Chem. Lett. 46 (2017) 1276–1284.
[21] P.V. Kamat, J. Bisquert, J. Buriak, ACS Energy Lett. 2 (2017) 904–905.
[22] C.M. Tsai, H.P. Wu, S.T. Chang, C.F. Huang, C.H. Wang, S. Narra, Y.W. Yang, C.L. Wang, C.H. Hung, E.W.G. Diau, ACS Energy Lett. 1 (2016) 1086–1093.
[23] T. Yokoyama, D.Y.H. Cao, C.C. Stoumpos, T.B. Song, Y. Sato, S. Aramaki, M.G. Kanatzidis, J. Phys. Chem. Lett. 7 (5) (2016) 776–782.
[24] C.K. Zhou, H.R. Lin, H.L. Shi, Y. Tian, C. Pak, M. Shatruk, Y. Zhou, P. Djurovich, M.H. Du, B.W. Ma, Angew. Chem. Int. Ed. 57 (2018) 1021–1024.
[25] C.K. Zhou, Y. Tian, M.C. Wang, A. Rose, T. Besara, N.K. Doyle, Z. Yuan, J.C. Wang, R. Clark, Y.Y. Hu, et al., Angew. Chem. Int. Ed. 56 (2017) 9018–9022.
[26] C. Zuo, L. Ding, Angew. Chem. Int. Ed. 56 (2017) 6528–6532.
[27] J.J. Snellenburg, S.P. Laptenok, R. Seger, K.M. Mullen, I.H.M. van Stokkum, J. Stat. Softw. 49 (2012) 1–22.
[28] I.H.M. van Stokkum, D.S. Larsen, R. van Grondelle, Biophys. Acta Bioenergy 1657 (2004) 82–104.
[29] M. Leng, Z. Chen, Y. Yang, Z. Li, K. Zeng, K. Li, G. Niu, Y. He, Q. Zhou, J. Tang, Angew. Chem. Int. Ed. 55 (2016) 15012–15016.

[30] G.S. Lorena, H. Hasegawa, Y. Takahashi, J. Harada, T Inabe, Chem. Lett. 43 (2014) 1535–1537.
[31] Y. Yamada, M. Hoyano, R. Akashi, K. Oto, Y. Kanemitsu, J. Phys. Chem. Lett. 8 (23) (2017) 5798–5803.
[32] H. Tang, F. Levy, H. Berger, P.E. Schmid, Phys. Rev. B 52 (1995) 7771–7774.
[33] I.A. Kudryavtseva, E.A. Vasil'chenko, A.C.C.B. Lush-chik, Phys. Solid State 41 (3) (1999) 388–395.
[34] P.B. Allen, I.B. Bischofs, Phys. Rev. B 65 (2002) 115113.
[35] J. Even, L. Pedesseau, C. Katan, M. Kepenekian, J.S. Lauret, D. Sapori, E. Deleporte, J. Phys. Chem. C 119 (19) (2015) 10161–10177.
[36] X.X. Wu, M.T. Trinh, D. Niesner, H.M. Zhu, Z. Norman, J.S. Owen, O. Yaffe, B.J. Kudisch, X.Y. Zhu, J. Am. Chem. Soc. 137 (5) (2015) 2089–2096.
[37] M.P. Hautzinger, J. Dai, Y.J. Ji, Y.P. Fu, J. Chen, I.A. Guzei, J.C. Wright, Y.Y. Li, S. Jin, Inorg. Chem. 56 (24) (2017) 14991–14998.
[38] R.L. Milot, R.J. Sutton, G.E. Eperon, A.A. Haghighirad, J.M. Hardigree, L. Miranda, H.J. Snaith, M.B. Johnston, L.M. Herz, Nano Lett. 16 (11) (2016) 7001–7007.
[39] D. Cortecchia, J. Yin, A. Bruno, S.Z.A. Lo, G.G. Gurzadyan, S. Mhaisalkar, J.L. Bredas, C. Soci, J. Mater. Chem. C 5 (2017) 2771–2780.
[40] J.M. Richter, M. Abdi-Jalebi, A. Sadhanala, M. Tabachnyk, J.P.H. Rivett, L.M. Pazos-Outón, K.C. Gödel, M. Price, F. Deschler, R.H. Friend, Nat. Commun. 7 (2016) 13941.
[41] L.M. Pazos-Outón, M. Szumilo, R. Lamboll, J.M. Richter, M. Crespo-Quesada, M. Abdi-Jalebi, H.J. Beeson, M. Vrućinić, M. Alsari, H.J. Snaith, B. Ehrler, R.H. Friend, F. Deschler, Science 351 (6280) (2016) 1430–1433.
[42] T. Hu, M.D. Smith, E.R. Dohner, M.J. Sher, X.X. Wu, M.T. Trinh, A. Fisher, J. Corbett, X.Y. Zhu, H.I. Karunadasa, A.M. Lindenberg, J. Phys. Chem. Lett. 7 (12) (2016) 2258–2263.
[43] M.D. Smith, H.I. Karunadasa, Acc. Chem. Res. 51 (3) (2018) 619–627.
[44] K. Thirumal, W.K. Chong, W. Xie, R. Ganguly, S.K. Muduli, M. Sherburne, M. Asta, S. Mhaisalkar, T.C. Sum, H.S. Soo, N. Mathews, Chem. Mater. 29 (9) (2017) 3947–3953.
[45] A.K.S. Song, R.T. Williams, Self-Trapped Excitons, Seconnd ed., Springer, Berlin, New York, 1996.
[46] T. Tokizaki, T. Makimura, H. Akiyama, A. Nakamura, K. Tanimura, N. Itoh, Phys. Rev. Lett. 67 (1991) 2701–2704.
[47] K.B. Zheng, K. Žídek, M. Abdellah, J.S. Chen, P. Chábera, W. Zhang, M.J. Al-Marri, T. Pullerits, ACS Energy Lett. 1 (2016) 1154–1161.
[48] J.M. Frost, L.D. Whalley, A. Walsh, ACS Energy Lett. 2 (2017) 2647–2652.
[49] D.B. Straus, S.H. Parra, N. Iotov, J. Gebhardt, A.M. Rappe, J.E. Subotnik, J.M. Kikkawa, C.R. Kagan, J. Am. Chem. Soc. 138 (42) (2016) 13798–13801.
[50] L. Lanzetta, J.M. Marin-Beloqui, I. Sanchez-Molina, D. Ding, S.A. Haque, ACS Energy Lett. 2 (2017) 1662–1668.